ORGANIC LETTERS

2011
Vol. 13, No. 19
5116–5119

Experimental and Theoretical Studies on the Radical-Cation-Mediated Imino-Diels–Alder Reaction

Raul Pérez-Ruiz,[†] Luis R. Domingo,[‡] M. Consuelo Jiménez,*[,†] and Miguel A. Miranda*[,†]

Departamento de Química-Instituto de Tecnología Química UPV-CSIC, Universidad Politécnica de Valencia, Camino de Vera s/n, 46022, Valencia, Spain, and Departamento de Química Orgánica, Universidad de Valencia, Dr. Moliner 50, E-46100 Burjassot, Valencia, Spain

mcjimene@qim.upv.es; mmiranda@qim.upv.es

Received July 22, 2011

ABSTRACT

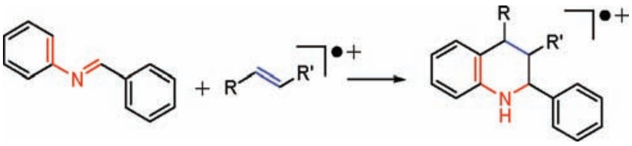

The feasibility of an electron transfer imino-Diels–Alder reaction between *N*-benzylideneaniline and arylalkenes in the presence of a pyrylium salt as a photosensitizer has been demonstrated by a combination of product studies, laser flash photolysis (LFP), and DFT theoretical calculations. A stepwise mechanism involving two intermediates and two transition states is proposed.

The acid catalyzed imino-Diels–Alder (IDA) reaction constitutes a highly active area of research,[1] from both the experimental[2] and theoretical[3] points of view. In fact, it is a widely employed strategy for construction of *N*-containing six-membered rings. Thus, IDA-based synthetic approaches lead to tetrahydroquinolines, which are found among natural alkaloids and biologically active compounds.[1e,f,4]

The electron transfer (ET) version of DA reactions, where the diene or the dienophile units are in the radical cationic form, has attracted considerable attention.[5] By contrast, the ET-mediated hetero-DA processes remain almost unexplored.[6] In this context, some IDA reactions have been achieved under assumed ET-conditions;[7] however, their mechanistic nature has not been elucidated, and

---

[†] Universidad Politécnica de Valencia.

[‡] Universidad de Valencia.

(1) (a) Cao, J.; Yang, X.; Hua, X.; Deng, Y.; Lai, G. *Org. Lett.* **2011**, *13*, 478–481. (b) Burland, P. A.; Coisson, D.; Osborn, H. M. I. *J. Org. Chem.* **2010**, *75*, 7210–7218. (c) Tambar, U. K.; Lee, S. K.; Leighton, J. L. *J. Am. Chem. Soc.* **2010**, *132*, 10248–10250. (d) Xie, M.; Chen, X.; Zhu, Y.; Gao, B.; Lin, L.; Liu, X.; Feng, X. *Angew. Chem., Int. Ed.* **2010**, *49*, 3799–3802. (e) Kouznetsov, V. V. *Tetrahedron* **2009**, *65*, 2721–2750. (f) Doyle, A. G.; Jacobsen, E. N. *Chem. Rev.* **2007**, *107*, 5713–5743.

(2) (a) Povarov, L. S. *Russ. Chem. Rev.* **1967**, *36*, 656–670. (b) Malassene, R.; Sanchez-Bajo, L.; Toupet, L.; Hurvois, J.-P.; Moinet, C. *Synlett* **2002**, 1500–1504. (c) Clerici, A.; Porta, O. *Tetrahedron Lett.* **1990**, *31*, 2069–2072. (d) Kobayashi, S.; Ishitani, H.; Nagayama, S. *Synthesis* **1995**, 1195–1202. (e) Yamanaka, M.; Nishida, A.; Nakagana, M. *Org. Lett.* **2000**, *2*, 159–161. (f) Hattori, K.; Yamamoto, H. *Tetrahedron* **1993**, *49*, 1749–1760. (g) Bortolotti, B.; Leardini, R.; Nanni, D.; Zanardi, G. *Tetrahedron* **1993**, *49*, 10157–10174. (h) Batey, R. A.; Simoncic, P. D.; Lin, D.; Smyj, R. P.; Lough, A. *Chem. Commun.* **1999**, 651–652. (i) Hadden, M.; Nieuwenhuyzen, M.; Osborne, D.; Potts, D.; Stevenson, P. J.; Thompson, N. *Tetrahedron Lett.* **2001**, *42*, 6417–6419.

(3) (a) Palacios, F.; Alonso, C.; Arrieta, A.; Cossio, F. P.; Ezpeleta, J. M.; Fuertes, M.; Rubiales, G. *Eur. J. Org. Chem.* **2010**, *11*, 2091–2099. (b) Ding, Y.-Q.; Fang, D.-C. *J. Org. Chem.* **2003**, *68*, 4382–4387. (c) Rodriguez-Borges, J. E.; Garcia-Mera, X.; Fernandez, F.; Lopes, V. H. C.; Magalhaes, A. L.; Cordeiro, M. N. D. S. *Tetrahedron* **2005**, *61*, 10951–10957.

(4) For some selected examples of the biological activity of tetrahydroquinolines, see: (a) Rauckman, B. S.; Tidwell, M. Y.; Johnson, J. V.; Roth, B. *J. Med. Chem.* **1989**, *32*, 1927–1935. (b) Witherup, K. M.; Ransom, R. W.; Graham, A. C.; Bernard, A. M.; Salvatore, M. J.; Lumma, W. C.; Anderson, P. S.; Pitzenberger, S. M.; Varga, S. L. *J. Am. Chem. Soc.* **1995**, *117*, 6682–6685. (c) Jacquemond-Collet, I.; Benoit-Vical, F.; Mustofa; Valentin, A.; Stanislas, E.; Malli, M.; Fourast, I. *Planta Med.* **2002**, *68*, 68–69.

(5) (a) Yueh, W.; Bauld, N. L. *J. Phys. Org. Chem.* **1996**, *9*, 529–538. (b) Fukuzumi, S.; Ohkubo, K.; Okamoto, T. *J. Am. Chem. Soc.* **2002**, *124*, 14147–14155. (c) Saettel, N. J.; Wiest, O.; Singleton, D. A.; Meyer, M. P. *J. Am. Chem. Soc.* **2002**, *124*, 11552–11559. (d) Fukuzumi, S.; Okamoto, T.; Ohkubo, K. *J. Phys. Chem. A* **2003**, *107*, 5412–5418. (e) Fürmeier, S.; Metzger, J. O. *J. Am. Chem. Soc.* **2004**, *126*, 14485–14492. (f) Gomez-Bengoa, E.; Helm, M. D.; Plant, A.; Harrity, J. P. A. *J. Am. Chem. Soc.* **2007**, *129*, 2691–2699.

10.1021/ol201984s

Scheme 1

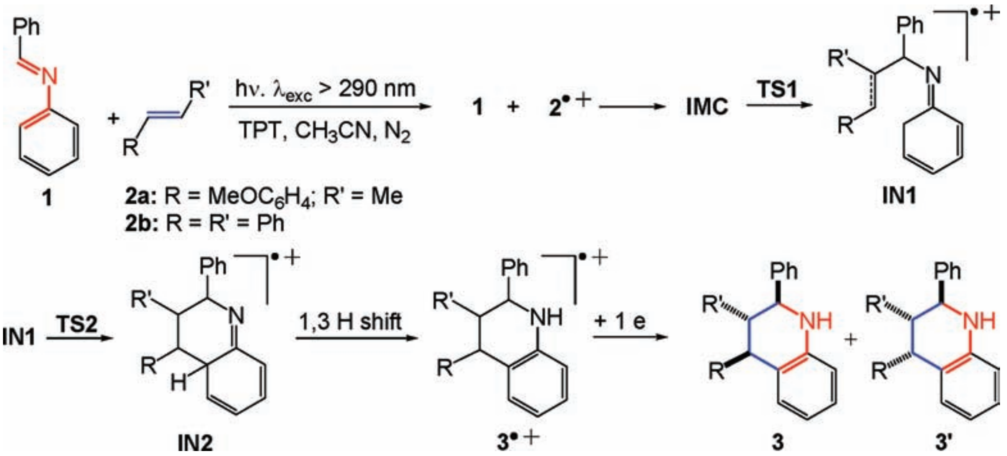

the involvement of radical cations as intermediates has not been proven.

To check the feasibility of IDA reactions proceeding through radical cationic species, *N*-benzylideneaniline (**1**) and *trans*-anethole (**2a**) were chosen as reaction partners and 2,4,6-triphenylpyrylium tetrafluoroborate (**TPT**) was chosen as an ET-photosensitizer.[8] The reaction has been analyzed by a combination of product studies, laser flash photolysis (LFP), and DFT theoretical calculations.

Acetonitrile solutions containing **1** (5×10^{-2} M) and **2a** (5×10^{-2} M) in the presence of catalytic amounts of **TPT** (5×10^{-3} M) were irradiated using the Pyrex filtered light of a 125 W medium-pressure mercury lamp (effective irradiation wavelength 290−500 nm) under N_2. The course of the photoreaction was followed by GC-MS. At 47% conversion, tetrahydroquinolines **3a** (85%) and **3′a** (15%) were isolated by HPLC as the only products (Scheme 1). Photolysis of **1** and **2a** under the same conditions, in the absence of **TPT**, led to recovery of unreacted starting materials.

The structural assignment of **3a** and **3′a** was based on MS, ^{1}H NMR, and ^{13}C NMR spectroscopy. Experimental details can be found in the Supporting Information (SI). Specifically, NOESY experiments (see SI, pp S6 and S14) were performed to establish the relative stereochemistry; they were consistent with a *trans, trans* configuration for isomer **3a** and a *trans, cis* configuration for **3′a**.The structure of **3a** was confirmed by X-ray analysis (Figure 1).

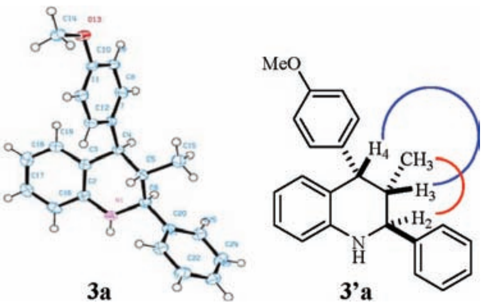

Figure 1. Left: X-ray structure of **3a**; right: NOE effects observed with **3′a**.

Estimation of the free energy change associated with ET from **2a** to the triplet excited state of the photosensitizer (^{3}**TPT***), using the Rehm−Weller equation[9] ($\Delta G_{ET} = -19$ kcal mol^{-1}), is compatible with generation of **2a**$^{\bullet+}$ in the initial step of the reaction.[10]

To obtain experimental evidence supporting involvement of the alkene radical cation, **TPT** was irradiated at 355 nm by LFP (MeCN/N_2) in the presence of increasing amounts of **2a**. As a matter of fact, the well-known ^{3}**TPT*** absorption[6,8] was quenched after addition of **2a**; the corresponding rate constant (k_q) was determined by means of the Stern−Volmer relationship;[11] it was found to be 1.6×10^{10} M^{-1} s^{-1}, indicating a nearly diffusion-controlled process (see SI, Figure S1).

Concomitantly with triplet quenching, two new bands were detected at 550 and 610 nm (Figure 2, top); they were safely ascribed to the pyranyl radical (**TPT**$^\bullet$) and *trans*-anethole

---

(6) (a) Argüello, J. E.; Pérez-Ruiz, R; Miranda, M. A. *Org. Lett.* **2007**, *9*, 3587–3590. (b) Domingo, L. R.; Pérez-Ruiz, R.; Argüello, J. E.; Miranda, M. A. *J. Phys. Chem. A* **2009**, *113*, 5718–5722.

(7) (a) Zhang, W.; Jia, X.; Yang, L.; Liu, Z.-L. *Tetrahedron Lett.* **2002**, *43*, 9433–9436. (b) Zhang, W.; Guo, Y. P.; Yang, L.; Liu, Z. L. *Chin. Chem. Lett.* **2005**, *16*, 575–578. (c) Zhou, Y.; Jia, X.; Li, R.; Liu, Z.; Liu, Z.; Wu, L. *Tetrahedron Lett.* **2005**, *46*, 8937–8939. (d) Zhang, W.; Guo, Y.; Liu, Z.; Jin, X.; Yang, L.; Liu, Z.-L. *Tetrahedron* **2005**, *61*, 1325–1333. (e) Jia, X.; Han, B.; Zhang, W.; Jin, X.; Yang, L.; Liu, Z.-L. *Synthesis* **2006**, *17*, 2831–2836. (f) Han, B.; Jia, X.-D.; Jin, X.-L.; Zhou, Y.-L.; Yang, L.; Liu, Z.-L.; Yu, W. *Tetrahedron Lett.* **2006**, *47*, 3545–3547.

(8) Miranda, M. A.; Garcia, H. *Chem. Rev.* **1994**, *94*, 1063–1089.

(9) Rehm, D.; Weller, A. *Isr. J. Chem.* **1970**, *8*, 259–271.

(10) Redox potentials of the donor and the acceptor (vs SCE): E_{ox}(**2a**) = 1.2 V; E_{red}(**TPT**) = −0.29 V; excited state energy: E_T(**TPT**) = 53 kcal mol^{-1}.

(11) *IUPAC Compendium of Chemical Terminology*, 2nd ed.; McNaught, A. D., Wilkinson, A., Eds.; Royal Society of Chemistry: Cambridge, 1997.

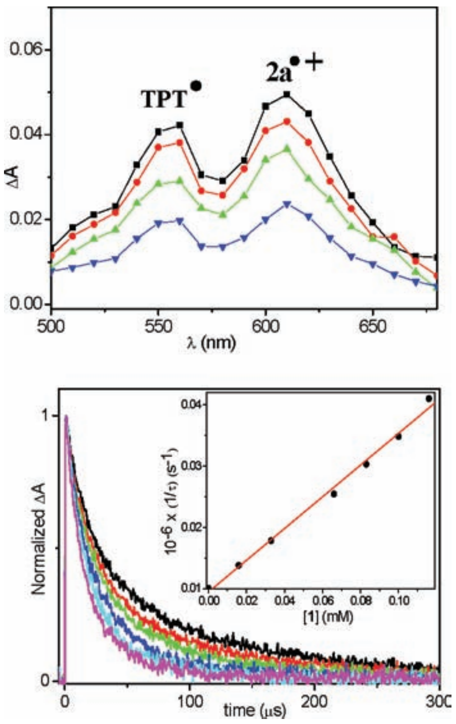

Figure 2. Laser flash photolysis (λ_{exc} = 355 nm, $MeCN/N_2$) of **TPT** (0.03 mM) and **2a** (0.30 mM). Top: Transient absorption spectra recorded 1 μs (■), 3 μs (●), 10 μs (▲), and 30 μs (▼) after the laser pulse. Bottom: Decay traces at 610 nm in the presence of increasing amounts of **1** (0.00–0.12 mM); inset: Stern–Volmer plot.

radical cation (**2a**$^{\bullet+}$), respectively, on the basis of literature data.[6,12] Simultaneous detection of the reduced form of the photosensitizer and the oxidized form of the alkene provided unequivocal support for the ET mechanism.

Having established the formation of radical cation **2a**$^{\bullet+}$ by LFP, the question arises whether the imine derivative **1** is capable of reacting with this intermediate, which would require direct quenching of **2a**$^{\bullet+}$ by **1**. In fact, addition of increasing amounts of **1** to **TPT**/**2a** mixtures resulted in a marked decrease of the **2a**$^{\bullet+}$ lifetime (Figure 2, bottom). Application of eq 1 allowed a k_q value of 2.6×10^8 M^{-1} s^{-1} to be obtained.

$$1/\tau = 1/\tau_0 + k_q[\mathbf{1}] \qquad (1)$$

We have previously found that *trans*-stilbene (**2b**) is essentially unreactive in related ET-mediated hetero-DA reactions with thiadienes,[6] due to delocalization of the spin and charge along the extended π-system. Indeed, when acetonitrile solutions containing **1**, **2b**, and **TPT** were submitted to steady-state irradiation under the usual conditions, not even traces of the possible IDA cycloadducts were detected.

In order to explain the above observations, the mechanistic aspects of the radical cationic version of the IDA reaction between **1** and **2a,b** were examined by means of DFT theoretical calculations at the (U)B3LYP/6-31G* level. Analysis of the potential energy surface (PES) indicated that the process occurs through a stepwise mechanism (Scheme 1). After generation of the radical cation **2**$^{\bullet+}$, the reaction proceeds through formation of an ion–molecule complex (**IMC**), which evolves to intermediate **IN1** *via* transition state **TS1**. In the subsequent step, ring closure occurs *via* **TS2** with formation of a new heterocyclic intermediate **IN2**. Finally, H shift affords the cycloadduct radical cation **3**$^{\bullet+}$. The intrinsic reaction coordinate (IRC) path was traced in order to check the energy profiles connecting each TS with the two associated minima of the proposed mechanism. Thus, IRC calculations at **TS1** and **TS2** led to localization of **IMC**s and **IN**s. Full optimization and subsequent frequency analysis confirmed that these species are minima on the PES. The relative

Table 1. Relative Energies[a] (ΔE, in kcal mol^{-1}) Obtained by B3LYP/6-31G*, in Gas Phase and Acetonitrile, for the Stationary Points Involved in the Radical-Cation-Mediated IDA Reaction between **1** and **2a**[b]

	gas phase	acetonitrile
IMCa	−10.1	−1.0
TS1a	8.0	17.3
IN1a	2.6	10.5
TS2a	15.6	21.3
IN2a	10.5	17.7
3a$^{\bullet+}$	−34.2	−30.8

[a] Relative to **2a**$^{\bullet+}$ + **1**. [b] See computational detais in the Supporting Information.

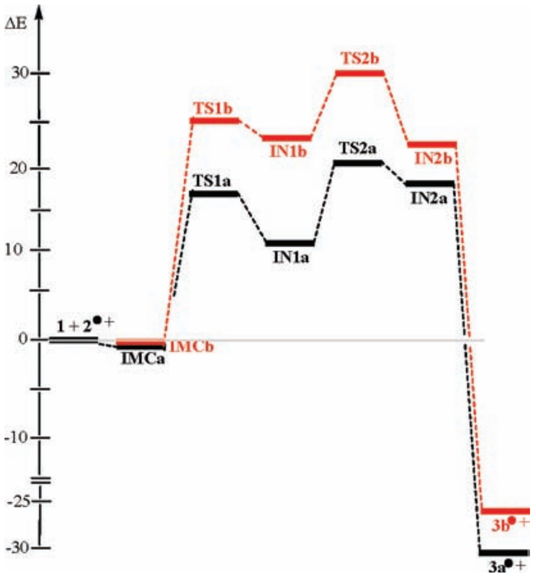

Figure 3. Relative energy profiles, in kcal mol^{-1}, for the radical-cation-mediated IDA reaction of **1** and **2a,b** in acetonitrile.

---

(12) Miranda, M. A.; Izquierdo, M. A.; Pérez-Ruiz, R. *J. Phys. Chem. A* **2003**, *107*, 2478–2482.

energies of the stationary points involved in the radical-cation-mediated IDA reaction between **1** and **2a** in acetonitrile are given in Table 1.

From the obtained relative energy profiles in acetonitrile (Figure 3) it seems clear that the overall activation energy for the formation of **IN2** is *ca.* 8 kcal mol^{-1} lower in energy for **2a** than for **2b**. This is in good agreement with the failure to detect IDA cycloadducts in the case of **2b**, for which the process is kinetically disfavored.

The geometries of the stationary points involved in the IDA reaction of **1** with **2a**$^{\bullet+}$ are shown in Figure 4. They are consistent with an asynchronous formation of the two new C$-$C bonds. The corresponding geometries of the stationary points for the reaction between **1** and **2b**$^{\bullet+}$ are given in the SI, Figure S4. Analysis of the natural atomic charges at **IMCa** indicates that the imine framework supports a positive charge of 0.27 e, while the alkene framework supports a positive charge of 0.73 e, indicating that at this stage some degree of charge transfer from **1** to **2a**$^{\bullet+}$ has taken place. Note that this charge reorganization also involves a parallel shift of the radical character between the two units. Although the small stabilization of **IMCa** in acetonitrile, compared to the reactants, is probably counterbalanced by entropic contributions, the charge and spin redistribution in this species provides an interesting insight into the electronic nature of the process.

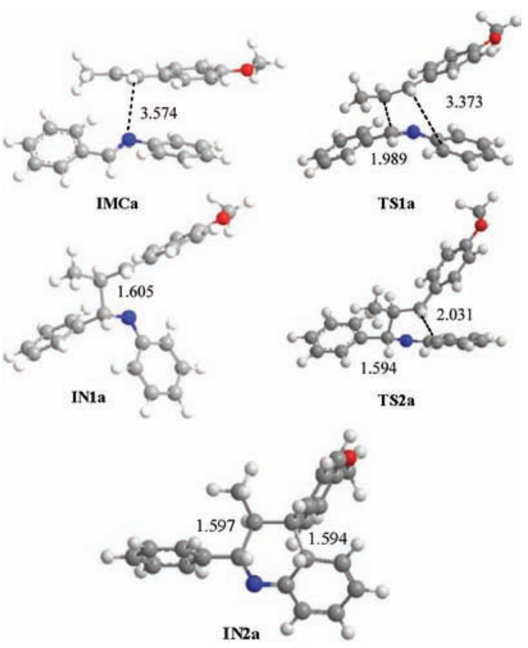

Figure 4. Structures of the ion$-$molecule complex, intermediates, and transition states of the radical-cation-mediated IDA reaction between **1** and **2a**.

For comparison, theoretical DFT calculations were also performed on the IDA reaction between **1** and **2a**, both in the nonionized form and in the acid-catalyzed counterpart. The results (see SI, Scheme S1, Tables S3 and S4, and Figures S2, S3, and S5) clearly show that the neutral version is kinetically disfavored with an activation energy higher than 35 kcal mol^{-1}. By contrast, upon acid catalysis the energy barrier becomes considerably reduced with a value of 16.5 kcal mol^{-1} in acetonitrile.

In summary, the feasibility of ET-mediated IDA cycloaddition has been proven by detection of the intermediate alkene radical cation, whose reaction with the imine partner can be followed in a microsecond time scale. According to DFT calculations, ionization of the alkene provides an effective catalytic strategy, although reduction of the energy barrier is somewhat less marked than in the well-known proton-assisted process.

Acknowledgment. Financial support from the MICINN (Grants CTQ2010-14882, CTQ2009-13699, CTQ2009-11027, and JCI-2010-06204) and from the UPV (Grant No. 20100994 and MCI Program) is gratefully acknowledged. Dedicated to Prof. Dr. Jaime Primo (Universidad Politécnica de Valencia) on the occasion of his 60th birthday.

Supporting Information Available. Additional experimental details; ^{1}H NMR, ^{13}C NMR, and phase-sensitive 2D NOESY of **3a** and **3′a**; X-ray structure and X-ray data of **3a** (CCDC 835816); reaction schemes; tables of the total and relative energies in gas phase and acetonitrile of the stationary points involved in the neutral, acid-catalyzed, and radical-cation-mediated IDA reaction between **1** and **2a**; table of the total and relative energies in gas phase and acetonitrile of the stationary points involved in the radical-cation-mediated IDA reaction between **1** and **2b**; geometries of the stationary points involved in several reactions; (U) B3LYP/6-31* Cartesian coordinates. This material is available free of charge via the Internet at http://pubs.acs.org.